Radio Pulsar Navigation System

João Maia Tomé
joao.maia.tome@tecnico.ulisboa.pt

Instituto Superior Técnico, Lisboa, Portugal

November 2022

Abstract

Navigation systems have been of common use for the past decades, but their development has been essential throughout history to map and locate new areas, as well as, moving safely between them. Currently, most of these systems rely on the Global Navigation Satellite Systems (GNSS), more specifically the Global Positioning System (GPS). However, these systems are not suitable outside their orbital sphere, inhibiting localization in outer space. Other navigation systems need to be explored for this application and that is what NASA and ESA are doing. The use of Pulsars is one of the new methods being explored, with the use of their extremely precise, unique and periodic signals. These signals have very weak power when received on Earth, lower than the noise level itself. Meaning that specialized hardware is required. With that, in this thesis, the partial development of a receiver suitable for this application is explored, using a quadratic receiver topology. More specifically, a 1 GHz frequency Gilbert cell mixer, with a switching current bias, and a relaxation oscillator implemented on a 65 nm CMOS technology. The oscillator has a frequency of 106 kHz, with an output amplitude of 0.6 V, centered at 1.9 V. The final circuit, simulated, obtained a constant output gain of 4.5 dB at the application frequencies, a bandwidth of 7.3 GHz, with a 1dB compression point of -9.5 dBm.
Keywords: Navigation System, Pulsar, Receiver, Mixer, Relaxation, Oscillator.

1. Introduction

Navigation systems have gone from physical maps used with compasses, later-on substituted by the astrolabe and the sextant. Which became obsolete or used only as a backup system due to the technological advancements in the last century, these have become obsolete, being replaced by the Global Navigation Satellite Systems (GNSS) with the common use worldwide of the Global Positioning System (GPS). Although very precise and extremely versatile on Earth, their utilization is limited to just that, the Earth. The satellites used are not available in outer space, meaning that navigation outside earth is not possible with such systems.

For outer space, spacecrafts currently rely on the observation of stars, with a base station on Earth acting as an observer, a reference and determining the route to be taken. This means that travelling in deep space is limited by the communication of the base station and the spacecraft, which currently are based radio and radar systems for both European Space Agency (ESA) European Space Tracking (ESTRACK) and National Aeronautics and Space Administration (NASA) Deep Space Network (DSN) [1].

The objective of this thesis is to make a specific component of an optimum receiver, shown in Figure 1, envisioned in [2] where a navigation system is proposed for outer space autonomous navigation using pulsars.

The main focus of this work is to develop the mixer (MXR) envisioned in the quadratic receiver topology proposed in Brito's PhD dissertation [2], with the local oscillator (LO) also being developed as a consequence. The whole proposed topology can be seen in Figure 1, with the section developed in this thesis highlighted in the dashed square in red.

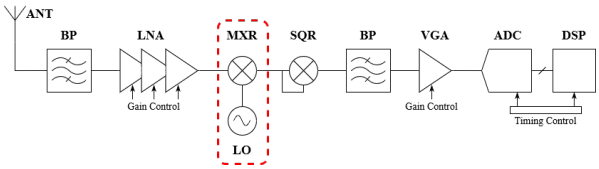

Figure 1: Proposed quadratic receiver topology in [2].

As such, the goal for this thesis is to develop a mixer for signals with a bandwidth of around 400 MHz at a center frequency of 1 GHz that will be used in the pulsar receiver, as well as, the 100 kHz oscillator that will be connected to the LO port of the mixer. For this, the TSMC65N technology is

used on the Cadence tool for development and simulation purposes.

Pulsars are pulsating stars, more specifically rapidly rotating neutron stars which magnetization emits beamed radio and other high energy radiation (X-ray to gamma-ray, figure 2). These were firstly discovered on November 1967, by Jocelyn Bell Burnell, with the discovery of a radio emitting pulsar named "PSR B1919+21". The radiation and the periodicity of pulsars' rotation makes their use ideal for navigation in deep space, especially with some specific pulsars [2]. This is a relatively new topic, with challenging means of detection, but that also means that new sources are discovered regularly.

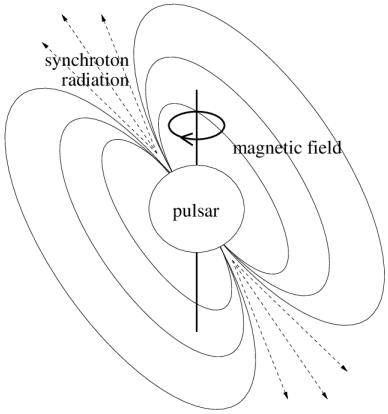

Figure 2: Pulsar model [3].

2. Background

In this section, the necessary background along with the state of the art theory in pulsars and mixers are presented. Some of the work already published in the areas of receivers and localization using pulsars is also presented.

2.1. Pulsar physics

What makes them exceptional for navigation and timing is their rotational period, which allows the extraction of extremely precise Time of Arrival (TOA) of radio signals, challenging even that of the atomic clocks' timing precision [4]. The main pulsars for this usage are those where the axis of rotation does not match the axis of radiation. That allows, just like a lighthouse, the radiation beam to be detected periodically. Luckily, about 90% of the known pulsars are in this category, with about 7% being millisecond pulsars, with periods ranging from 1.5 to 30 ms [5]. Millisecond pulsars are capable of maintaining their period for billions of years [6]. These are the desirable pulsars for navigation, not only for their longevity, but because their position, relative to the Solar System Barycenter (SSB), can be acquired precisely in less time. Currently there are about 530 of these pulsars registered in the "ATNF Pulsar Catalogue" [7].

To obtain the TOA, we must first have an understanding of the pulsar rotation. The rotational phase of the pulsar in relation to a given time t is given by

$$\phi(t) = \phi(t_0) + f(t - t_0) + \frac{1}{2}\dot{f}(t - t_0)^2 + ... \quad (1)$$

with rotational frequency as

$$f = \frac{d\phi}{dt}, \quad (2)$$

where t_0 is a given reference epoch, and $\dot{f}$ is the first derivative of f [8]. This lets us determine the minor deviations on the pulse timing compared to the expected signal timing from the SSB and adjust the TOA.

2.2. Pulsar Signal

The challenging aspect of using pulsars for navigation is the detection of their signal (pulse). Thankfully, each pulsar has a unique profile, allowing the distinction between them, as shown in figure 3. The known profiles are of high precision, allowing to accelerate the time it takes to identify a specific pulsar signal, by means of correlation.

The signal is challenging to detect due to the low power that is received at the detector. This means that the pulses are undetectable with a single sample, as the noise is at a higher power level than the pulse itself. In order to improve their detection, several techniques can be employed at hardware level, such as low noise receivers to maximize the already low signal-to-noise ratio (SNR) and at a post-processing level, by employing folding with the desired time periods and with the aid of correlation in case there are several pulsar signals mixed in the receiver. These techniques are mainly used for the observation and detection of new pulsars.

The signal of the pulsar, at the source, can be mathematically perceived using the model presented in (3) [10]. The model for the signal is

$$s_p(t) = a(t) \cdot p(t) = a(t) \cdot \sum_{n=-\infty}^{\infty} p(t - nT_p), \quad (3)$$

having the pulsar signal as two separate components, $a(t)$ which is a natural random process, in this case a zero-mean real Gaussian, caused by the synchrotron radiation, and the deterministic signal $p(t)$ which is related to the pulsars rotation at period T_p. Figure 4 is a representation of these signals. Since $a(t)$ is stationary, this results in a cyclostationary pulsar signal, with an average period of T_p.

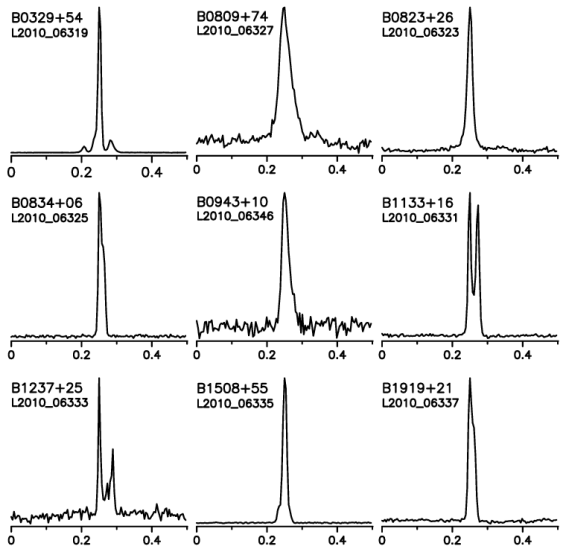

Figure 3: Pulse profile for nine different pulsars [9].

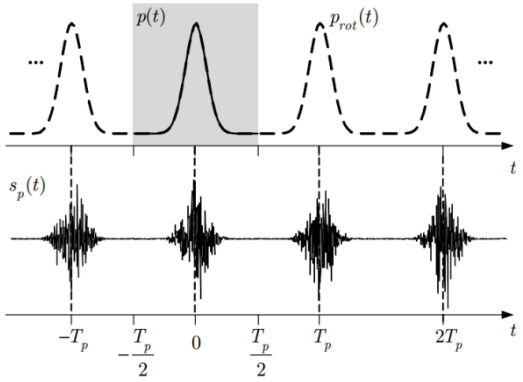

Figure 4: Model for $s_p(t)$ and $p(t)$ [10].

Having understood the model of the signal, the important aspects to acquire the signal are the SNR and the frequency spectrum. In relation to the latter, pulsars have a wide range of frequencies, with the most likely candidates in the radio frequencies, X-rays or γ-rays. The use of the high energy pulsars like the X-ray and γ-rays seems logical, since it improves the SNR, but not only are the receivers more complicated and unpractical [11], these pulsars represent only a small portion of the known pulsars to date, with the first γ-ray pulsars only being discovered recently [12]. Radio frequency pulsars are more common, with easier topologies for the receivers, but that comes at a loss of the SNR.

2.3. Pulsar Receiver

Taking into consideration the SNR obtained from 15 suitable radio frequency pulsars, as shown in Figure 5, the center frequency of the receiver is best around the 1 GHz mark [10], to maximize the SNR, since most of the pulsars peak around that frequency. Even with this, the desired signal of all the pulsars is well below the -40 dB mark compared to the noise.

Once again, this is a big hurdle for the detection of pulsar signals. The need to detect signals below the noise level leads to the development of low-noise receivers, used in conjunction with several data processing techniques. As mentioned before, this thesis focuses on the quadratic receiver topology proposed by Brito. This architecture focuses on the use of a squarer after the initial low-noise amplifier (LNA), which allows the small bandwidth of the received signal (pulsar signal and noise) to be squared and shifted to the direct current (DC) region. The advantage of this methodology, since the signal bandwidth is in the few hundreds of kHz, is the possibility of using a better performing analog-to-digital converter (ADC), with a reduced sampling frequency and high resolution, which is one of the most important features of the architecture.

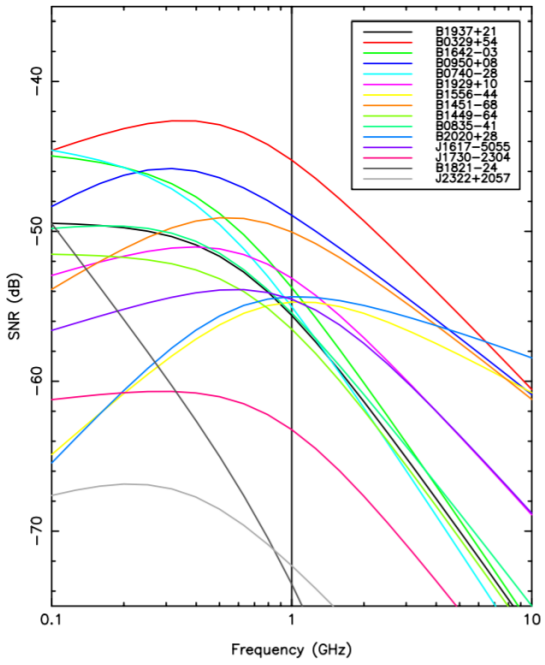

Figure 5: SNR as a function of frequency for 15 pulsars, with $A_e = 10$ m^2 [13].

The usage of a squarer presents drawbacks that will be explained later on. One solution to mitigate those drawbacks is to implement a frequency mixer in order to cause a shift to the original signal. Since this thesis focuses on this part of the receiver, in the next section, the functionality and technological advancements of mixers are presented.

2.4. Mixers

Mixers are an essential building block for a receiver. Their function is to perform frequency translation by multiplying two waveforms.

In their basic form, frequency mixers are composed of three distinct ports: radio frequency (RF), LO and intermediate frequency (IF). When used as a down-conversion mixer, the RF port is the input signal, the LO port is where the oscillator is connected and the IF port is the output with the two frequencies mixed.

One way to categorize different mixers is based on the circuitry used. They can be passive or active. Passive mixers use passive components, or active components in a passive region, for the switching element in the RF part, such as diodes or saturated transistors. They are known as switching mixers and don't consume any DC power. Their use is limited by their inability to have gain, since there is no transconductance stage, and their limited frequency response. As for active mixers, these use transistors, in a transconductance stage, and can provide gain as well as the mixing of the two signals.

Since the transconductance stage is the major contributor for non-linearity, passive mixers are not affected by it, since even if they have MOSFET transistors as switches, they are ideally in the triode region. This means that, usually, passive mixers have better linearity than active mixers.

Mixers can also be categorized by whether they are single-balanced or double-balanced. Non-balanced mixers, or single-ended mixers, are not used in current day RF circuits.

In order to compare different mixers, the Figure of Merit (FOM) in (4) is useful to have an idea of the relative performance taking into consideration the most important aspects of the mixer [14]. The FOM for mixers is given by:

$$FOM = 10 \cdot \left(\frac{10^{\mathrm{Gain}/20} \cdot 10^{(\mathrm{IIP3}-10)/20}}{10^{\mathrm{NF}/10} \cdot P_{MIX}(\mathrm{mW}) \cdot 10^{-3}} \right), \quad (4)$$

where Gain is the mixer's conversion gain, IIP3 is its input third-order intercept point, NF is the noise factor of the mixer and P_{MIX} is the mixer power.

Another important metric is the conversion gain compression, more specifically the 1 dB compression point. This is the input power point where the output signal starts showcasing amplitude distortion and the mixer loses its linearity. The 1_{dB} compression point is defined as the input RF power required to have a conversion loss of 1 dB from ideal [15].

2.5. Double-Balanced Mixers

As mentioned before, one way to categorize frequency mixers is if their inputs and outputs are balanced or not. Since double-balanced mixer designs have a better isolation between the ports, their use is ideal for an application with low input power and with noise constraints.

The circuit in figure 6 is a Gilbert Cell mixer, the most generally used type of mixer. Since it is a double-balanced mixer, it has a differential transconductance stage in addition to the differential switching stage. The gain is applied on the RF signal, while the other four transistors are switching both modulated currents from the first stage. In order to have good switching, the transistors in the first stage must be considerably bigger than the four switching transistors.

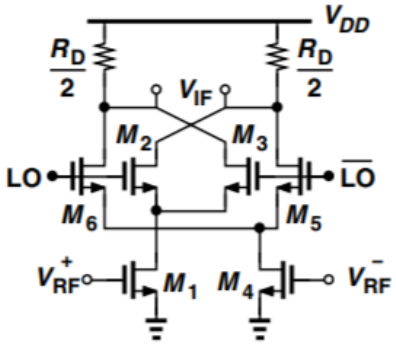

Figure 6: Gilbert Cell mixer topology [16].

The use of source degeneration with an inductor can improve the linearity of the design, although with an impact to the NF [17]. For example in [18], the Gilbert Cell topology is implemented with an inductive degenerated source, common mode inductor and the gates of the transistors also have an inductive load, while also biasing it at the minimum NF current density bias. This, and the fact that an IF buffer is present and impedance matched to 50 Ω, lowers the total noise and is shown to improve linearity[18].

Another case is the design developed in [19], where the resistive output load is exchanged for an LC tank designed to resonate at the desired frequency of 5 GHz, allowing for an improved headroom and the control of the output bandwidth depending on its quality factor. A common source inductor is used, just like in [18], for common mode rejection of imbalances inherent to asymmetries. An inductor is also placed between each switching pair and the transconductance stage pair to improve the conversion gain, since they minimize parasitic capacitances.

Although it greatly improves noise and gain, this type of circuit is impractical for small technology sizes and applications, since the use of several inductors means a significant area increase. Ideally,

these benefits are achieved without the need for big area passive components.

2.6. Switching Tail Current Bias

A major point of introduction of noise to the circuit is the tail current source. A technique used to mitigate this is presented in [20] and [21], with the use of a switching current bias.

This is achieved by having two MOSFETs controlled by each of the IF components. With this, the tail current transistors are constantly changing between strong inversion and accumulation regions, allowing for trapped charge carriers to be released [20]. Therefore, the flicker noise is reduced. In Figure 7, this implementation is shown by the use of transistors M1 and M2. Additionally, the transistors M11 and M12 are used as DC shifters. This is needed for the higher voltage of the output to be able to effectively regulate the biasing transistor that is activated.

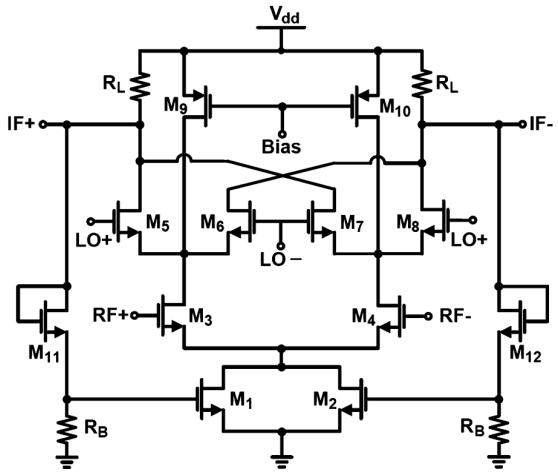

Figure 7: Gilbert Cell mixer with switching tail current bias [20]

Compared to the previous noise reducing design, there is only two resistors as extra passive components. Since it uses no inductors or capacitors, it is able to take advantage of a slightly lower noise input without a big impact on circuit size.

3. Relaxation Oscillator

A typical relaxation oscillator is composed of a couple of cross-coupled inverters, a current source for each, two resistive loads and an integrating capacitor, as shown in Figure 8.

In such oscillator, each inverter is active independently. As the current is integrated, the voltage across the capacitor rises, leading to the latching of the inverters and switching the inverter that is active. After this, the capacitor is discharged, leading to the latch back to the original inverter.

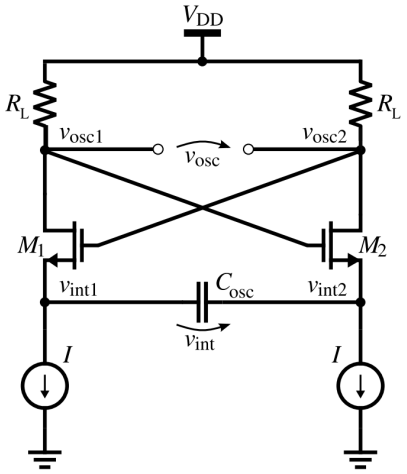

Figure 8: Example of CMOS relaxation oscillator [22].

This constant oscillation behaviour is tuned by the size of the resistive load and the capacitor [22], with an approximate frequency of

$$\mathrm{f}_{osc} = \frac{1}{8 \times \mathrm{C}_{osc} \times \mathrm{R}_L}, \tag{5}$$

while the amplitude is dependent on the resistive load and the current sources. Since the circuit switches periodically with latches, the output waveform is a differential square waveform.

Concluding, in order to obtain an oscillation frequency of the desired magnitude for the LO, the passive components require unreasonably large values for the technology used. To prevent this and still be able to use this topology of oscillator, the resistors can be switched for transistors in the triode region, allowing the tuning of its internal resistance to a greater value than a resistor, while having significantly lower area. By doing this, the size of the capacitor can also be lowered, granting the ability of having a low frequency oscillator, with reduced area size, on a nm scale technology.

4. Implementation

4.1. Mixer Design

Taking into account the necessities of this receiver, the mixer developed in this thesis focuses on a low noise application, with good isolation between the ports. Since pulsar signals have a center frequency of 1 GHz, that should be the desired center frequency of the RF port. As for the LO port the desired frequency is 100 kHz. This is because the receiver topology employs a squarer, and the desired pulsar signal should be kept out of its flicker noise region. As the bandwidth of the desired pulsars is lower than 100 kHz, mixing the pulsar signal frequency with the local oscillator will allow it to shift

and be kept out of the DC levels of the squarer output. The double balanced mixer, or Gilbert cell, is ideal for this situation. Not only does it have a lower noise floor, but it also has excellent isolation between the ports with its differential inputs and outputs.

The design and simulation of this circuit can be divided in several stages. For initial simplicity's sake, the circuit is tested with an RF input at 1 GHz and the LO frequency of 100 MHz. This allows for better simulation and tuning of the device since it drastically reduces the simulation time, compared to the desired specification of 100 kHz for the LO frequency. After the initial design process, the frequency is switched to the desired specification.

4.2. Input Biasing

In order to have the possibility of connecting any source signal to the input ports, a circuit that blocks the DC component of that source and biases it to the voltages needed for each stage's transistors, mentioned in table 1, is implemented.

Table 1: Input DC voltages.

Input	Voltage (V)
VDD	2.5
LO	1.8
RF	1.3

In order to do the biasing internally, a transistor with the drain and the gate shorted is implemented. This gives a constant voltage output dependant on the size of the transistor and the current input. For the input signal to be filtered a high pass filter is used, in the way of a series capacitor, to block the DC component. This method is shown in figure 9.

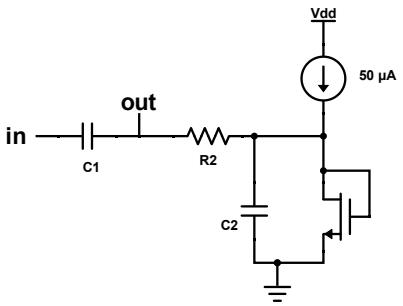

Figure 9: Biasing transistor.

In order to only have one external current to provide the biasing for the MOSFETs, therefore reducing the external components, cascading this voltage reference circuit seems feasible, as the bias voltage for the transconductance stage is lower than for the switching stage. However, the current from one input signal that influences the I_D current in the MOSFET, and therefore its voltage drop, would also influence the current in the MOSFET for the other signals, reducing the signal to noise ratio, since there would be leakage from one input port to the other. Because of this the inputs biasing filter consists of four independent voltage references, two for the RF port (one for each complementary signal of the differential source) and the other two for the LO port (one for each complementary signal of the differential input of the LO).

This circuit will only be applied to the RF ports, since the desired LO frequency presents additional challenges with this filter, due to parasitic capacitance of the transistors. For the LO port, an oscillator biased at the mentioned bias voltage is developed later on.

4.3. Switching Mixer Current Bias

To minimize the noise while also keeping the circuit area minimal, the switching tail current bias technique is used, as seen in [20] and [21]. In addition to the switching MOSFETs, four other MOSFETs are used in order to shift the output voltage to the threshold of the bias MOSFETs. This can be seen in figure 10.

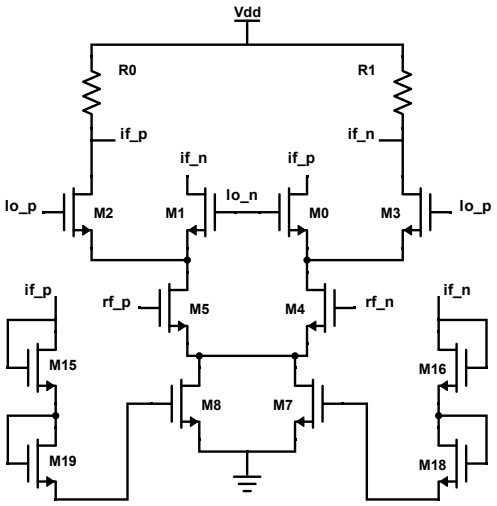

Figure 10: Mixer adapted with the switching bias.

4.4. Relaxation Oscillator

To counter the LO biasing blocking the signal at the desired frequency for the oscillator, the integration of a simple, slow (for this technology size) relaxation oscillator is proposed. The final schematic implemented is shown in figure 11, with transistors M5 and M11 acting as a resistive load to allow a higher impedance than a size limited resistor.

Since the output of an oscillator of this topology is a square wave, to minimize the impact of the harmonics on the input of the mixer, an RC low-pass filter is implemented with a cutoff frequency at

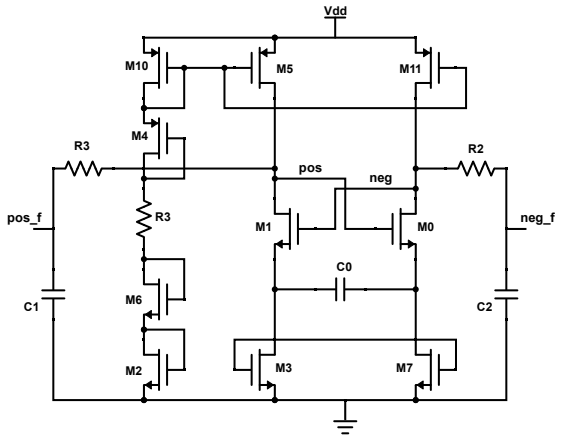

Figure 11: Relaxation oscillator schematic.

200 kHz. Since the oscillator is tuned for 100 kHz, this filter minimizes the first odd harmonic (since it is a squared wave) by 6 dB.

4.5. Final Design

The finished circuit has the relaxation oscillator developed as the LO input of the mixer adapted with the switching bias, and the DC biasing transistor for the RF port input. The addition of the oscillator allows the mixer to work at the intended frequency, without the need for filtering at the LO port, since the correct voltage bias is already set by the oscillator. This leads to the use of a biasing filter only at the RF port, where there is minimal loss of AC signal since the input frequencies are much higher than the filter cut-off frequency.

5. Results

In this section, the simulated results of the various development phases for each component are presented. The metrics of the whole system are also presented at the end.

5.1. Mixer at High LO Frequency

Simulating the circuit shown in figure 10 with a transient, the correct functionality of the mixer is verified. Table 2 summarizes the defined values of the design variables used for the simulation.

Table 2: Transient simulation variables

Variable	Value
V_{LO}	500 mV
V_{RF}	10 mV
f_{LO}	100 MHz
f_{RF}	1 GHz

The simulated results for the mixer, including the input filters and the switching bias, can be seen in figure 12. A slight attenuation of the RF is present, due to the biasing circuit. The LO signal also is affected by this attenuation but, later on, with the addition of the developed oscillator, this is not present anymore. The IF output has the two sinusoidal waves with the two frequencies visible.

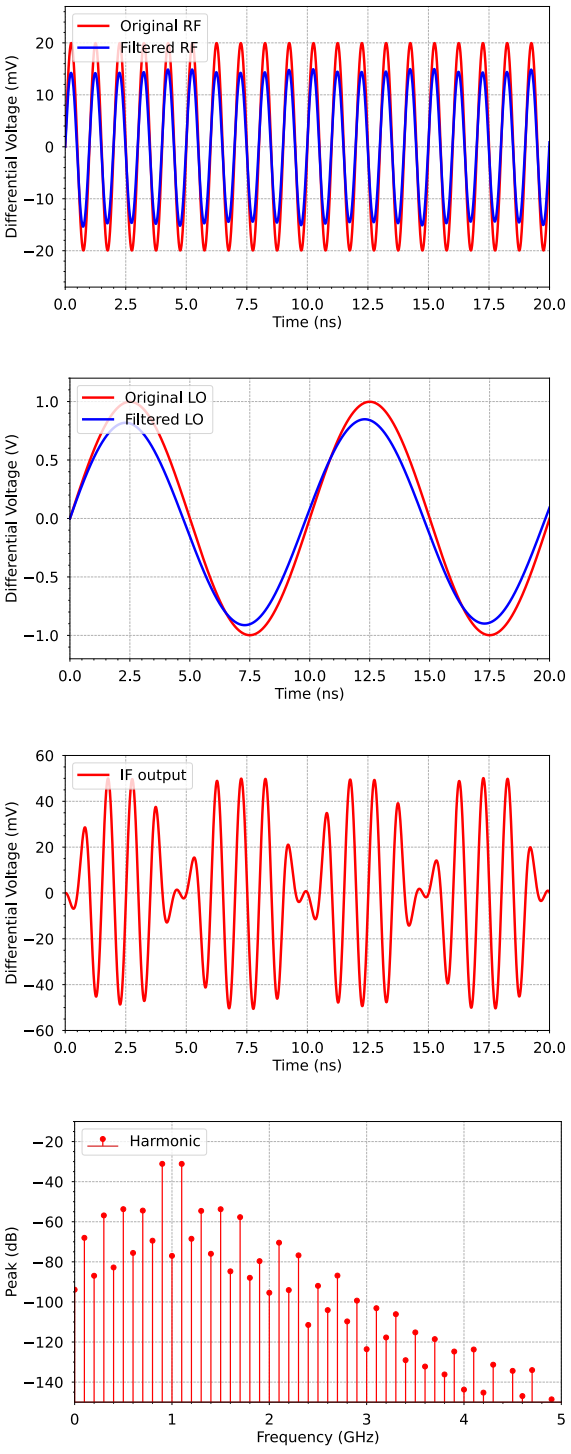

Figure 12: Mixer transient simulated response

The arbitrary voltage for the LO must be optimized. To determine the LO amplitude for maximum gain, a voltage sweep is performed. From

figure 13 it is visible that the 0.5 V used is close to the maximum gain of the circuit designed, just below the 3 dB figure.

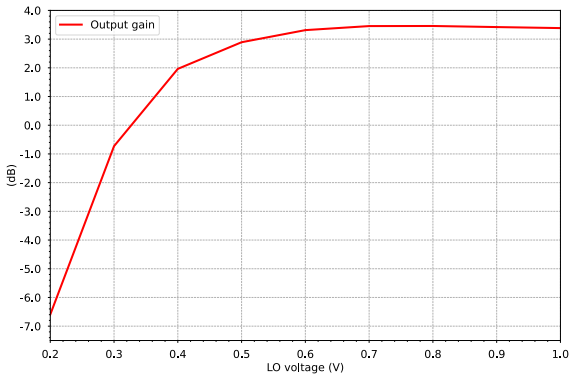

Figure 13: Mixer gain in function of LO voltage amplitude.

With a functional circuit at high LO frequencies, in order to function with the mixer at low LO frequencies, the development of the oscillator is necessary, as was mentioned in the previous section. The simulation results for the oscillator circuit will be presented next.

5.2. Oscillator

From the transient simulations of the oscillator circuit, analyzing a single-ended output in figure 14, it can be observed that the oscillator is tuned to an amplitude of 0.6 V centered at 1.9 V, to allow the switching transistors of the mixer to function in the correct operating region. The frequency is also at a value of 106 kHz.

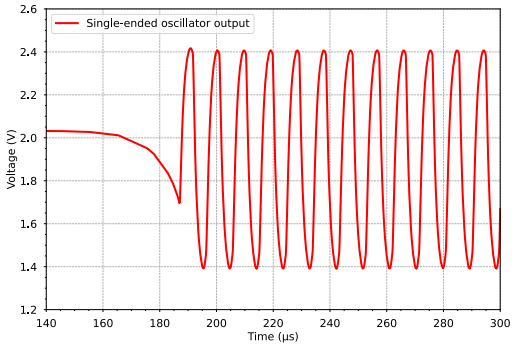

Figure 14: Relaxation oscillator single-ended output voltage.

Performing a Monte Carlo simulation with 200 runs, the mean frequency continues at the 106 kHz mark, but with a standard deviation of 23 kHz. Although undesirable, such variation in frequency due to production and mismatch will not affect the final functionality of the mixer. That is because the signal from the pulsar is not a sine wave, but a periodic pulse. The objective of the mixer is just to shift this signal a few kHz out of what will be the squarer's DC output. Therefore, a frequency deviation of around 20 kHz at the oscillator, leads to a deviation on the shift caused by the mixer to the RF port. Although, even if the shift to the pulsar signal is a 80 kHz or a 120 kHz shift, it will still keep the signal out if the flicker noise region generated at the squarer's transistors and the band-pass filter following the squarer (figure 1) can be tuned to cope with this shift as well.

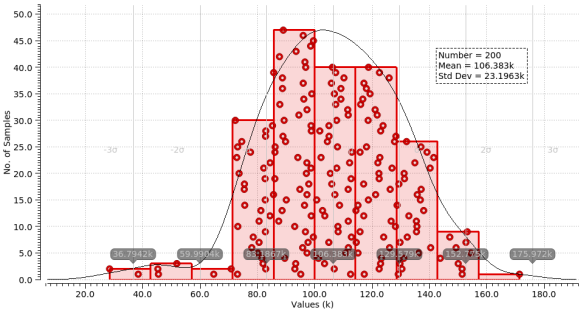

Figure 15: Relaxation oscillator frequency Monte Carlo.

The Fast Fourier Transform (FFT) shown in figure 16, shows the difference in output waveform due to the RC filter, where the third harmonic is -16 dB in relation to the 100 kHz harmonic, 6 dB lower than the circuit without a filter.

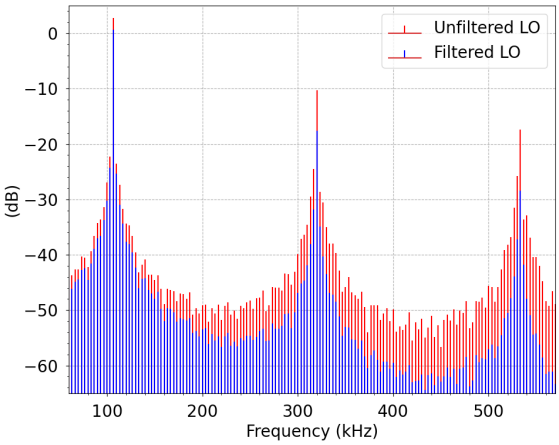

Figure 16: FFT of RC filter influence on relaxation oscillator.

5.3. Final Circuit

Connecting the relaxation oscillator directly to the LO port of the frequency mixer without the biasing filter before the switching pair transistors, the circuit is on its final form. From the simulation of the output gain in relation to the frequency, shown

in figure 17, the final circuit obtained a maximum gain of 4.5 dB, with a bandwidth of 7.3 GHz. The maximum gain is centered at the 1 GHz mark, as desired.

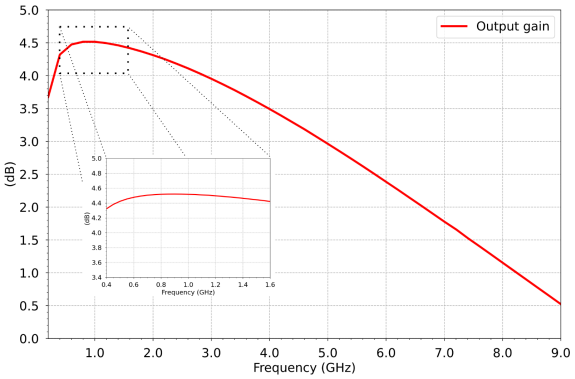

Figure 17: Circuit output gain and bandwidth.

The 1_{dB} compression point of the circuit is simulated to -9.5 dBm, as shown in figure 18, meaning that the input power can reach that value before the output gain decreases by 1 dB. Since the pulsar signals will be of very reduced power, this result is well within the desired specifications. While the expected use of this receiver is with pulsar signals with power below the noise level, the 1_{dB} compression point result obtained allows for the future possibility of using the circuit at closer ranges to the pulsars than expected.

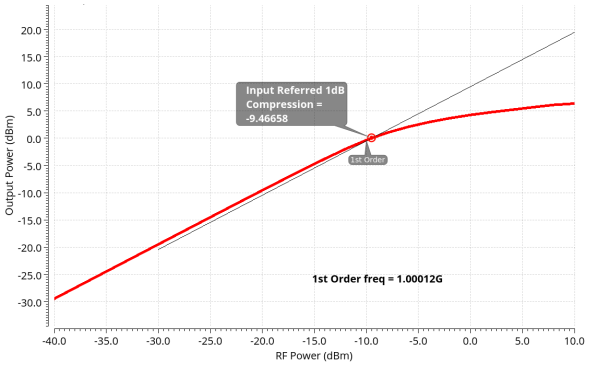

Figure 18: Circuit 1_{dB} compression point.

Although the simulations were simplified by using the pulsar input as sine waves, the results obtained demonstrate that the circuit is able to mix two signals with different magnitudes of frequency, at a low power level and with a gain of 4.5 dB. These specifications were obtained through several iterations and tuning cycles, obtaining a mixer and local oscillator that can be integrated into the receiver envisioned in [2].

6. Conclusions

The desire and importance of outer space navigation are undeniable to understand the universe and explore its contents. The use and development of new localization and navigation systems is essential to allow better and further exploration. The benefit of pulsars for this application is still a relatively new research area, but with promising results.

In order to take advantage of pulsar signals for navigation, the development of capable receivers is necessary. The work proposed for this thesis, a mixer and oscillator for a quadratic receiver topology, was achieved.

The Gilbert Cell mixer with switching current bias developed achieves a gain of 4.5 dB, 1_{dB} compression point of -9.5 dBm. The 7.3 GHz input bandwidth makes it suitable for the application, especially since the maximum gain is constant at the pulsar signal's frequency. As for the relaxation oscillator, it boasts an amplitude of 0.6 V and a frequency of 106 kHz. The development of these topologies at these frequencies was quite challenging for a small and fast technology such as the TSMC65N.

This result allows the squarer of the receiver to perform its objective without introducing flicker noise to the pulsar signal. Since the mixer is able to function correctly with both inputs having frequencies orders of magnitude apart, the desired shift of the pulsar signal by a few 100 kHz allows the ADC to have a higher resolution. Such objective was the main difficulty of this project, which, although functional, still has some deviation on the oscillator frequency. Even though it does not affect the functionality of the final product, it implies some extra steps at the data processing stage.

The presented results validate the proposed topologies but some improvements in hardware are still possible. An external interface to regulate the relaxation oscillator's capacitance could minimize the frequency deviation. For future work, the fabrication layout and simulation should also be finalized. The integration of the squarer into this design should be analyzed, as it may allow the reduction of conversions between current and voltage. Finally, the rest of the receiver can be implemented as a single tape-out integrated circuit.

Acknowledgements

Firstly, I would like to give a very special thanks to both of my supervisors, Professor Jorge Fernandes and Doctor Diogo Brito, for their time, support and knowledge in developing this work. I am grateful for the opportunity to work in a project thesis of this area.

I am also grateful to Instituto Superior Técnico (IST) and INESC-ID for the facilities and condi-

tions that permitted the continuous development of this thesis.

The work developed in this thesis was also supported by FCT, Fundação para a Ciência e a Tecnologia (Portugal), under the projects UIDB/50021/2020, UNSEEN - PTDC/EEI-EEE/31416/2017; and FCT/EU Moore4Medical - H2020-ECSEL-2019-IA-876190.

I would also like to thank my family and friends for supporting me throughout my academic studies. Especially my parents and my brother, who continuously give me strength to reach my goals.

References

[1] Sami Asmar, Daniel Firre, Andrea Accomazzo, Alaudin Bhanji, Paolo Ferri, John Hudiburg, Phil Liebrecht, Gary Morse, and Gregory Mann. NASA's and ESA's Tracking Networks, A Decade of Strategic Partnership for Solar System Exploration. *2018 SpaceOps Conference*, 2018.

[2] Brito, Diogo. *Radio Pulsar System for Navigation.* PhD thesis, Instituto Superior Técnico, 2018.

[3] Stefan Rüster. *The Phase Diagram of Neutral Quark Matter.* PhD thesis, December 2006.

[4] Demetrios Matsakis, J. Taylor, and Marshall Eubanks. A Statistic for Describing Pulsar and Clock Stabilities. *Astronomy and Astrophysics*, 326, Septemper 1997.

[5] Andrew Lyne and Francis Graham-Smith. *Pulsar Astronomy.* Cambridge Astrophysics. Cambridge University Press, 4 edition, 2012.

[6] Ryan S Lynch. Pulsar Timing Arrays. *Journal of Physics: Conference Series*, 610, may 2015.

[7] Australia Telescope National Facility. The ATNF Pulsar Catalogue, 2022.

[8] Diogo Brito, Gonçalo Tavares, Jorge Fernandes, Arash Noroozi, and C.J.M. Verhoeven. Radio Pulsar Receiver Systems for Space Navigation. 2015.

[9] J. Hessels, B. Stappers, A. Alexov, T. Coenen, T. Hassall, A. Karastergiou, V. Kondratiev, M. Kramer, J. Leeuwen, J.J.D. Mol, A. Noutsos, and P. Weltevrede. Early Pulsar Observations with LOFAR. Septemper 2010.

[10] João Santos, Diogo Brito, Gonçalo Tavares, and Jorge Fernandes. Radio Pulsar Signal Generator. In *2018 IEEE International Symposium on Circuits and Systems (ISCAS)*, 2018.

[11] Suneel Ismail Sheikh. *The use of variable celestial X-ray sources for spacecraft navigation.* University of Maryland, College Park, 2005.

[12] The Fermi LAT Collaboration. An extremely bright gamma-ray pulsar in the Large Magellanic Cloud. *Science*, 350, 2015.

[13] Josep Sala-alvarez, Andreu Planas, J. Villares, Robert Estalella, and Joshi Paredes. Feasibility Study for a Spacecraft Navigation System relying on Pulsar Timing Information. 01 2004.

[14] Mustafijur Rahman and Ramesh Harjani. A Sub-1-V 194-μW 31-dB FOM 2.3–2.5-GHz Mixer-First Receiver Frontend for WBAN With Mutual Noise Cancellation. *IEEE Transactions on Microwave Theory and Techniques*, 64, 2016.

[15] C. Marki and F. Marki. Mixer Basics Primer. Technical report, 2010.

[16] Behzad Razavi. *Rf Microelectronics.* Prentice Hall, 1998.

[17] Keng Leong Fong and R.G. Meyer. Monolithic rf active mixer design. *IEEE Transactions on Circuits and Systems II: Analog and Digital Signal Processing*, 46, 1999.

[18] K.W. Tang, M. Khanpour, P. Garcia, C. Garnier, and S.P. Voinigescu. 65-nm cmos, w-band receivers for imaging applications. In *2007 IEEE Custom Integrated Circuits Conference*, 2007.

[19] David Alldred, Brian Cousins, and Sorin P. Voinigescu. A 1.2v, 60-ghz radio receiver with on-chip transformers and inductors in 90-nm cmos. In *2006 IEEE Compound Semiconductor Integrated Circuit Symposium*, 2006.

[20] Jong-Ha Kim, Hee-Woo An, and Tae-Yeoul Yun. A low-noise wlan mixer using switched biasing technique. *IEEE Microwave and Wireless Components Letters*, 19, 2009.

[21] Shasanka Rout and Kabiraj Sethi. Design of high gain and low noise cmos gilbert cell mixer for receiver front end design. 2016.

[22] Ortigueira, Eduardo. *Low Phase-Noise CMOS RC Oscillator for RF Applications.* PhD thesis, Universidade Nova de Lisboa, 2018.